Observation of two-hole satellite in the resonant x-ray photoemission spectra of $Ba_{1-x}K_xFe_2As_2$ single crystals

A. Koitzsch,[1] R. Kraus,[1] T. Kroll,[1] M. Knupfer,[1] B. Büchner,[1] H. Eschrig,[1] D. R. Batchelor,[2] G. L. Sun,[3] D. L. Sun,[3] and C. T. Lin[3]

[1]*Institute for Solid State Research, IFW Dresden, P.O. Box 270116, D-01171 Dresden, Germany*

[2]*Forschungszentrum Karlsruhe GmbH, Institut für Synchrotronstrahlung, ISS, Herrmann-von-Helmholtz-Platz 1, D-76344 Eggenstein, Germany*

[3]*Max-Planck-Institute for Solid State Research, Heisenbergstraße 1, D-70569 Stuttgart, Germany*

(Received 31 March 2010; published 20 May 2010)

We probe the correlation regime of $Ba_{1-x}K_xFe_2As_2$ single crystals by x-ray photoemission spectroscopy. Although the data explicitly confirm the itinerant character of the electrons, the satellite features observed at the L_3 threshold indicate at the same time local behavior. This dichotomy suggests that, although the pnictides appear to be unusually weakly correlated, local electronic excitations cannot be neglected for the correct description of the material.

DOI: 10.1103/PhysRevB.81.174519 PACS number(s): 74.25.Jb, 74.70.−b, 79.60.−i

I. INTRODUCTION

The recent discovery of superconductivity in the iron oxypnictides with maximum $T_c=56$ K (Refs. 1 and 2) is a surprising and important event and may trigger significant progress in the field of superconductivity. The electronically active parts of the crystal structure are the FeAs layers. On the one hand it is surprising that iron is beneficial for superconductivity and on the other hand it puts the pnictides in a prominent row of transition-metal (TM) compounds with their inherent richness of physical phenomena. The driving force for the latter are correlations, i.e., large on-site repulsion energies U. How important are they for the pnictides? This question is the starting point for every basic description as well as advanced theoretical modeling. In this paper we investigate in detail the correlation regime of the pnictides, which has been much disputed recently. Proposals spawn the full range from weakly[3,4] via moderately[5] to strongly[6,7] correlated systems. Most of them are based upon spectroscopic evidence, especially x-ray spectroscopy.[8–11]

The main subject of this paper and a well-known consequence of strong correlations are satellite features in the photoemission spectra. A stringent way to uncover such satellites is $2p$-$3d$ resonance photoemission because the resonance enhancement is much stronger in the satellite than in the main line. Such experiments have led to the assignment of the satellites in, e.g., the cuprates,[12] nickelates,[13] and iron oxides[14,15] but also for elemental Ni,[16,17] Fe and Cr,[18] and Cu metal.[19] Here, we apply resonant photoemission and develop a consistent view on the entire photoemission results. We confirm explicitly small values of U and find, nevertheless, clear signatures of local electronic excitations. Basic properties of the material are not understood, e.g., the magnetic moment comes out much too large in theory—both in the local approach with a high spin state due to small crystal-field splitting but also for the various density-functional-theory schemes. A natural speculation is then that the value of the moment is due to a complex interplay or competition between both extremes. To substantiate this speculation hard evidence is needed that local excitations are present and which energetics they follow.

II. METHODS

Photoemission and absorption experiments have been performed at the BESSY undulator beamline UE-52 PGM equipped with a Scienta R4000 analyzer and drain current measurement. The total energy resolution was set to 220 meV for $h\nu=700$ eV and to 420 meV for $h\nu=1000$ eV. The base pressure during measurements was better than $p=5\times10^{-10}$ mbar. The single-crystalline samples have been cleaved *in situ* before the measurements at room temperature. The energies are referenced to the Fermi edge of sputtered gold. Undoped $BaFe_2As_2$ (BFA) and slightly underdoped single-crystals $Ba_{1-x}K_xFe_2As_2$ (BKFA) ($T_c=32$ K, $x=0.3$) were grown using Sn flux in a ZrO_2 crucible.[20]

The total density of states (DOS) and projected DOS (PDOS) were obtained from the all electron full-potential code FPLO8.[21]

III. RESULTS AND DISCUSSION

A. Off-resonant valence band

Figure 1 shows the valence bands of BFA and BKFA for a wide range of photon energies. We observe the typical pnictide valence band reported before with a peak below $E=-1$ eV and a flat-structured plateau region extending till $E=-6$ eV for $h\nu=150$ eV which evolves into a broad peak with several shoulders as the photon energy increases. The difference to previous studies on polycrystalline samples is that the low-energy peak is much enhanced here. The lower panels of Fig. 1 show the calculated DOS. The DOS has been obtained within the local density approximation (LDA). According to theory the low-energy peak is almost exclusively due to Fe $3d$ whereas at higher energies As $4p$ contributes substantially. This is in agreement with experiment: at $h\nu=150$ eV the Fe $3d$ cross section is 40 times larger than for As $4p$ but for 1500 eV the ratio changes to 1.3.[22] In each panel we compare the experimental spectrum with a cross

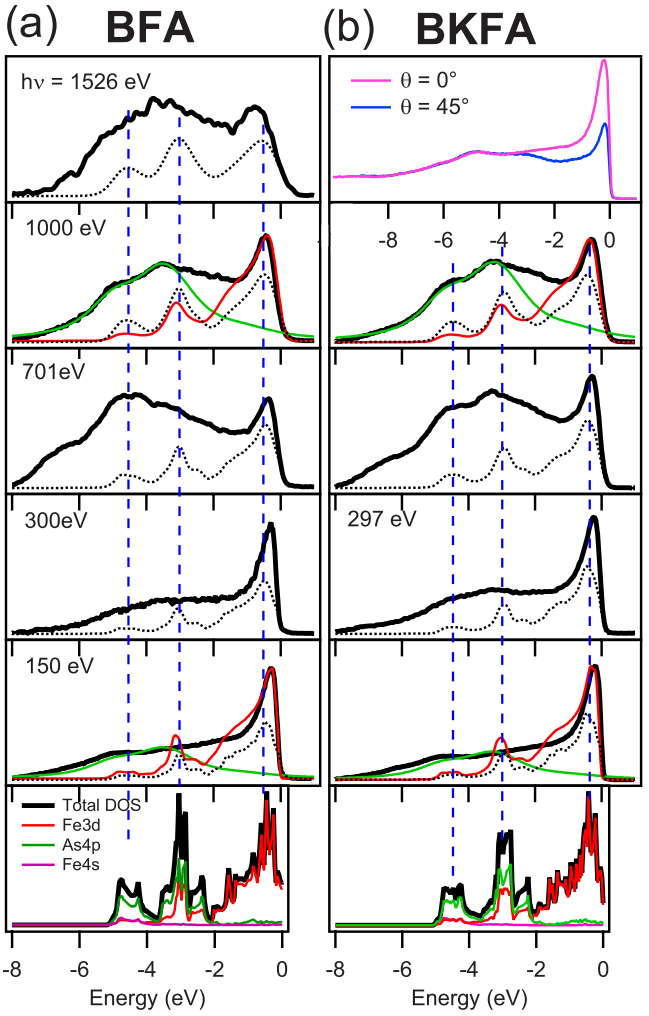

FIG. 1. (Color online) Comparison of experimental (thick black) valence bands of (a) $BaFe_2As_2$ and (b) $Ba_{1-x}K_xFe_2As_2$ with cross-section-weighted DOS calculations (black dotted lines) and modeled partial spectra of As $4p$ (green, centered at E≈−4 eV) and Fe $3d$ (red, centered at E≈−0.5 eV) (see text). The upper panel of (b) shows an emission angle dependence for $h\nu$=150 eV. θ is the angle relative to the surface normal. The lower panels show DOS calculated based on a LDA calculation. A Shirley background has been subtracted from the black experimental spectra. Blue dashed lines are guides to the eye.

section weighted DOS convolved with a lorentzian (FWHM=0.05 eV) to account for the lifetime of the photohole and a Gaussian to simulate finite resolution. This simple approach reproduces the main features but (i) underestimates the spectral weight between −2 and −5 eV, and (ii) underestimates the broadening between −2 and −5 eV while overestimating it below −2 eV. To achieve a better, i.e., more quantitative, agreement between experiment and theory regarding the line shape we drop the artificial assumption of an energy and orbital-independent hole lifetime. For the Fe $3d$ states we introduce a phenomenological Kramers-Kronig consistent self-energy of the form $\Sigma(E)=-gE/(E+i\Gamma)^2$ and calculate the partial Fe $3d$ spectrum according to

$$A(E) = 1/\pi \int d\varepsilon \cdot N(\varepsilon)\mathrm{Im}[E-\varepsilon-\Sigma(E)]^{-1} \qquad (1)$$

(Ref. 9). The results for g=0.4 eV^2 and Γ=1 eV are shown by the red, solid lines in the 150 and 1000 eV panels folded with 80 and 400 meV Gaussian broadenings, respectively. The parameters have been chosen so as to fit the low-energy peak of the Fe $3d$ PDOS. They result in moderate absolute values of the self-energy ($\mathrm{Re}\,\Sigma_{\max}$=100 meV, $\mathrm{Im}\,\Sigma_{\max}$=200 meV) but still underestimate the broadening at higher energies. The As $4p$ partial DOS, on the other hand, is folded with a lorentzian of FWHM of 0.8 eV (green line) and shifted toward higher energies by 0.35 eV. The agreement between the green line and the spectra is remarkable. Note that the tail of the green line extending to unoccupied states is an artifact of the energy-independent broadening. Between E=−2 eV and −5 eV the Fe $3d$ and As $4p$ states are hybridized according to the calculation, and their PDOS has a similar shape. Therefore, a similar large broadening of the Fe $3d$ states as applied for the As $4p$ states in that energy region would improve the agreement regarding the overall lineshape. However, the spectral weight is more difficult to reconcile with theory: At $h\nu$=150 eV the spectrum is totally dominated by the Fe $3d$ emission due to the low As $4p$ cross section. Considering this, the spectral weight of the Fe $3d$ PDOS above E=−2 eV is much too small compared to experiment. The ratios of the integrated spectral weight between E=0 and −2 vs E=−2 and −8 for experiment and theory for $h\nu$=150 eV are 0.95 and 2.74, respectively. LDA underestimates the spectral weight at high energies by a factor of 3.

For a layered single-crystalline solid, such as the pnictides, the spectral weight of a given orbital depends not only on the cross section but also on its vicinity to the surface and its orientation relative to the polarization vector of the incoming beam. The top panel of Fig. 1(b) shows an emission angle dependence of the valence band. The Fe $3d$-related emission below E=−2 eV goes down as the angle is increased whereas the higher energy part remains constant. This is consistent with the presence of the As layer at the surface because the As $4p$ PDOS is located mainly above E=−2 eV. However, for the present measuring geometry, the polarization is completely in plane for the 45° spectrum, whereas it has on out-of-plane component for the 0° spectrum, which enhances emission.

In terms of the spectral weight ratio between high and low energy the disagreement between theory and experiment even worsens for 45° emission. Assuming the As layer at the surface does not remove this discrepancy: with a distance of the Fe and As layer of 1.4 Å (Ref. 23) and a mean-free path of the photoelectrons of ~5 Å at 150 eV (Ref. 24) the intensity of the As emission is enhanced compared to Fe only by a factor of approx 1.3. Since the As $4p$ emission is suppressed by a factor of 40 compared to Fe $3d$ due to the photoemission cross section, the total spectral weight is practically still that given by the Fe $3d$ PDOS. It has been shown previously that LDA+U schemes cause a transfer of spectral weight from low to high energies accompanied by a narrowing of the low-energy line shape.[6] This fits qualitatively the

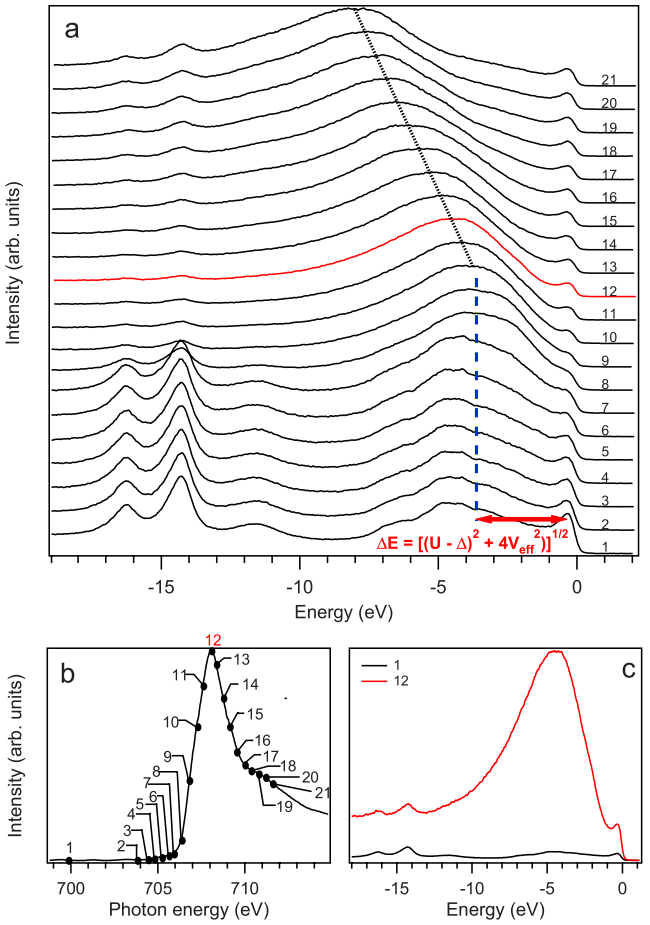

FIG. 2. (Color online) (a) Resonance profile of the valence band of $BaFe_2As_2$. The spectra are normalized to maximum. The blue dashed line tracks the resonant intensity enhancement at $E=-3.6$ eV, the black dotted line the Auger emission. (b) Fe L_3 absorption edge. The numbers correspond to the energies of the valence-band spectra. (c) Spectra 1 and 12 replotted from (a) normalized to the Ba 5p peak area.

above observations and explicitly introduces correlation effects in the discussion. To investigate the physical consequences of the latter in more detail, we consider resonance photoemission in the next section.

B. On-resonant valence band

The resonance enhancement of satellite structures is essentially a local effect. It enhances the emission from the orbitals of the absorbing edge by a coherent superposition of direct photoemission of the type $3d^n \rightarrow 3d^{n-1}+e^-$ and a Super Coster-Kronig-type Auger process $2p^6 3d^n \rightarrow 2p^5 3d^{n+1} \rightarrow 2p^6 3d^{n-1}+e^-$, where e^- stands for the outgoing photoelectron. Both processes lead to equivalent final states and interfere.

Figure 2(a) shows a series of valence-band spectra taken with excitation energies across the Fe $2p$-$3d$ transition as indicated in the absorption scan shown in Fig. 2(b). The spectra are normalized to maximum in Fig. 2(a) to emphasize the photon-energy dependence of the energy position of the valence-band features. The absolute intensity enhancement on resonance is substantial as can be seen in Fig. 2(c), where off- and on-resonant spectra are normalized to the shallow core levels. Before the resonance (position 1) the valence-band spectra is dominated by the normal photoemission process. The Ba $5p$ core levels are situated betwwen $E=-14$ eV and $E=-17$ eV. The small peak at $E\approx-11.5$ eV is due to As $4s$. For spectra 2–10 we find sharp intensity increase centered at the blue dashed line ($E=-3.6$ eV). The fact that no energy shift is present in this region indicates that the enhancement is driven by the radiationless resonance Raman process[25] and characterizes the peak as the two-hole satellite.[10,18] Starting from spectrum 11 we find an energy shift of the resonance emission toward higher energies, indicating that the incoherent Auger process prevails. The strong resonance enhancement at $E=-3.6$ eV is reminiscent of the enhancement of the satellite intensity in other TM compounds.

The resonance enhancement occurs in the energy region of the valence band that is insufficiently described by the LDA alone, i.e., where spectral weight is missing by a large margin. A natural assumption is that the appearance of the spectral weight in experiment is driven by correlation effects, which redistributes spectral weight to higher energies. In an extreme case, such us pure Mott Hubbard materials like the cuprates, a distinct satellite peak appears at high energies. Based on Fig. 2 we argue that satellite intensity is present for the pnictides as well but, due to the small values of U, intermixed with the normal valence band.

For a more quantitative estimation of the correlation regime at work we apply a simple two-level interaction model,[26] where the splitting between the d^5- and d^6L-dominated levels becomes

$$\Delta E = \sqrt{(U-\Delta)^2 + 4V_{\mathrm{eff}}^2}, \tag{2}$$

where U is the Hubbard repulsion, Δ the charge transfer energy, and V_{eff} the effective hopping parameter for tetrahedral symmetry. We apply our previously extracted data set from the analysis of the Fe L_3 absorption edge [$U=1.5$ eV (multiplet averaged), $\Delta=0$, $V_{\mathrm{eff}}=1.5$ eV (Ref. 27)] and obtain $\Delta E=3.4$ eV.[28] If we consider the Fe $3d$-derived peak near E_F at $E=-0.35$ eV as the well screened state (d^6L) the satellite (d^5) is expected around $E=-3.7$ eV in remarkable agreement with experiment.

For a metallic, largely itinerant system, such as the pnictides, the two-level model is a rather drastic approximation. However, local models have been successfully applied before to analyze the electronic structure of the pnictides[3,9] and we use only parameters from an independent measurement. Also the crystal structure itself implies in some sense a local approach: the Fe-Fe distance in BFA is 2.8 Å and the Fe-As distance only 2.4 Å, with very large As $4p$ orbitals in a tetrahedral "closed-packed" local environment of every Fe site. Of course, the strong directional overlap of the Fe $3d$ states provides the basis for the metallic, itinerant behavior of the system.

To scrutinize the resonance process in more detail, Fig. 3 presents color-coded summary plots of the resonance enhancement as a function of photon energy for the undoped and doped compounds. The presentation in Fig. 3 aims to

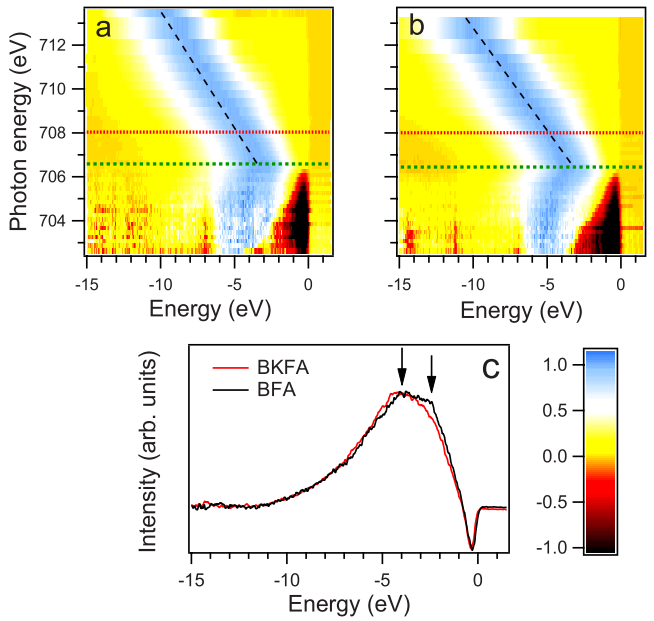

FIG. 3. (Color online) [(a) and (b)] Valence band as a function of photon energy for (a) BFA and (b) BKFA. A Shirley background has been removed, and the off-resonant spectra, normalized to the Ba $5p$ lines, have been subtracted out. The resulting difference spectra are normalized to maximum to emphasize the dispersion. Red dotted lines highlight the position of the absorption maximum (E_{XAS}), green dotted lines of the Fe $2p_{3/2}$ binding energy. (c) Horizontal cuts from (a) and (b) at $h\nu$=706.4 eV. Arrows highlight the fine structure of the BFA spectrum.

emphasize the resonance behavior. To this end the off-resonant valence-band spectrum (labeled 1 in Fig. 2) has been subtracted from all on-resonant valence bands after normalization to the Ba $5p$ levels. Then each resulting spectrum has been normalized to maximum in order to enhance the visibility of the photon-energy dependence of the resonance features. Figures 3(a) and 3(b) contain also the energy of the absorption maximum (E_{XAS}) (red dotted line) and the binding energy of the Fe $2p_{3/2}$ core level (E_{XPS}) (green dotted line; see also Fig. 4). Below E_{XPS} the energy position of the features is constant or slightly bent to lower energies indicating the appearance of new features. Above E_{XPS} and clearly before E_{XAS} the peak shifts to higher energies and assumes a Auger-type dispersion. The color scale in Fig. 3 has been set to highlight intensity suppression by red and black. Interestingly the energy region where intensity suppression is found increases linearly starting at $h\nu=|E_B|$ for decreasing $h\nu$. For $h\nu<|E_B|$ a fine structure appears in the resonance profile, which is unrelated to the DOS. Figure 3(c) shows a direct comparison of doped and undoped spectra for $h\nu$ below the onset of the Auger dispersion. The undoped spectrum has sharp structures whereas the doped has no. Such sharp structures in the resonance regime are consistent with the presence of multiplet states in the satellite.

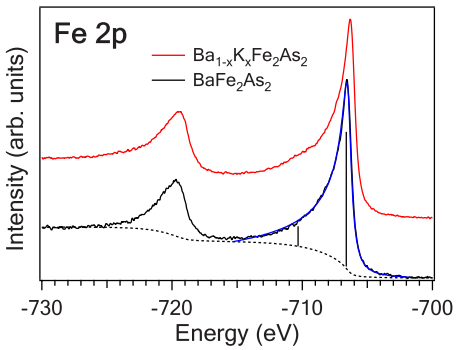

FIG. 4. (Color online) Fe $2p$ core levels of $Ba_{1-x}K_xFe_2As_2$ taken with $h\nu$=1000 eV. The dotted line is a Shirley background. Bars represent the results of the two-level-configuration model (see text). The blue line is the result of a Doniach-Sunjic fit (without background).

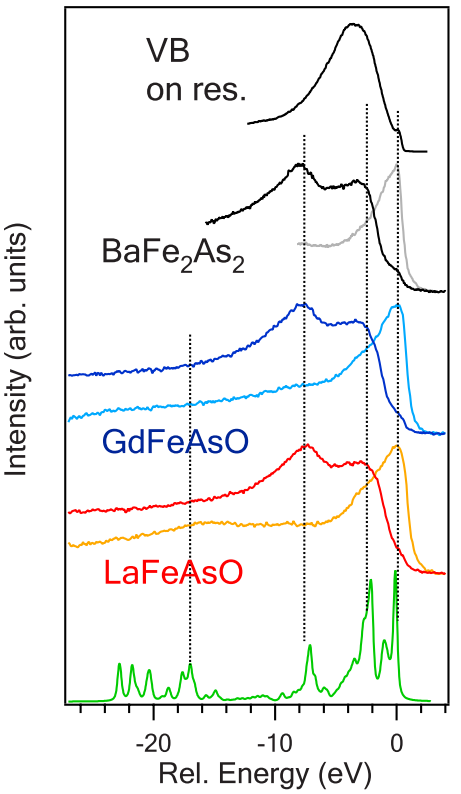

FIG. 5. (Color online) Fe $3p$ core levels of $BaFe_2As_2$, GdFeAsO, and LaFeAsO measured off (gray, light blue, orange) and on (black, blue, red) the Fe L_3 resonance in comparison with the valence band of $BaFe_2As_2$. The spectra are aligned to the lowest-energy peaks.

The observed resonance behavior resembles the one found in elemental iron[18] but is not identical. The resonance maximum is shifted to higher binding energies for the pnictides in comparison to iron (E=−3.6 vs −3.2 eV), and the energy difference between E_{XPS} and E_{XAS}, which is associated with the correlation regime, has a larger value for the pnictides than pure iron (1.4 vs 0.9 eV).[18] This reflects the different bonding of the iron atoms in the pnictides, in particular, the hybridization with the As—tetraeder surrounding each Fe—atom.[10]

C. Core levels

Figures 4 and 5 complement the discussion of the valence

band by the Fe $2p$ and $3p$ core levels. Figure 4 shows the Fe $2p$ line for BFA and BKFA measured with $h\nu=1000$ eV. The line has two spin-orbit split components corresponding to Fe $2p_{3/2}$ at $E=-706.6$ eV and Fe $2p_{1/2}$ at $E=-719.7$ eV. The shape of the Fe $2p_{3/2}$ lines is asymmetric at the high-energy side but no apparent satellite features are observed, consistent with previous reports.[9,27,29] The BFA spectrum was fitted with a Doniach-Sunjic line shape appropriate for simple itinerant metals.[30] The asymmetry parameter assumes high values ($\alpha=0.46$) consistent with previous reports and typical for d-metal screening.[29,31] At the bottom of the figure the two-level interaction model with the same parameters as used above for the valence band is presented, with $\Delta E=\sqrt{(U_{dc}-\Delta)^2+4V_{eff}^2}$, where U_{dc} is the core-level repulsion, which we have set to $U_{dc}=U+1$ eV and V_{eff} adjusted for the correct number of holes in the d shell. We adopt the view that the charge-transfer multiplets are completely screened by the metallic charge carriers. The line shape of the Fe $2p$ line is therefore dominated by the metallic response of the system and hardly shows any fine structure related to satellites or multiplets. Resonance photoemission is not possible for the $2p$ line itself but it is possible for the $3p$ line. The Fe $3p$ core levels of single-crystalline BFA and polycrystalline LaFeAsO and GdFeAsO (Ref. 27) are presented in Fig. 5 off- and on-resonant (i.e., measured with photon energies corresponding to the maximum of the L_3 absorption edge). The off-resonant Fe $3p$ line has a small spin-orbit splitting and, similar to the Fe $2p$ lines, an asymmetric overall line shape. Contrary to the Fe $2p$ line, fine structures are recognizable even in the off-resonant data: a small shoulder at $E=-2.8$ eV and intensity increase at $E=-8$ eV are present at the high-energy side (dashed lines). On resonance these structures are strongly enhanced, whereas the main line is not and appears small, similar to the valence band in resonance which is reproduced in the figure for comparison.

The experimental data in Fig. 5 are compared with the result of a charge-transfer-multiplet calculation at the bottom.[32] The calculation uses two initial states as a basis (d^6 and d^7L) and takes into account charge transfer to the ligand As tetraheder and atomic multiplet splitting. We used again exactly the same parameters as for the x-ray absorption spectroscopy, the valence band and the Fe $2p$ line. We find qualitative agreement between experiment and theory. All experimental features have their theoretical analogon.

The Fe $3p$ excitation shows clear signs of satellite emission both off- and on-resonance. It is, therefore, dominated by local effects, contrary to the Fe $2p$ line which is dominated by Donjach-Sunjic-type screening. The latter would probably have to be taken into account for a more quantitative description of the Fe $3p$ line as well. The fact that the Fe $3p$ spectra can be described using only two configurations as a basis justifies also partly the even more simple two-level-configuration ansatz used for the valence band.

IV. SUMMARY

Looking at the entirety of the results the picture of a weakly correlated material emerges, for the description of which one-particle theory is an appropriate starting point. This ansatz reproduces the valence band on a semiquantitative level and the core levels show the typical asymmetric line shape of metallic screening. However, for the full analysis of the valence band and the core levels local effects have to be taken into account. Our parametrization of the observed satellite enhancement yields excellent agreement to experiment with a multiplet averaged value of $U=1.5$ eV. Despite this small value local electronic excitations exist in the pnictides and influence the properties of the material.

ACKNOWLEDGMENTS

This project was supported by the DFG under Grants No. KN 393/12 and No. KR 3611/1-1. We thank R. Hübel, R. Schönfelder, and S. Leger for technical support and J. Fink for helpful discussions. We acknowledge the Helmholtz-Zentrum Berlin–Electron storage ring BESSY II for provision of synchrotron radiation.

[1] Y. Kamihara, T. Watanabe, M. Hirano, and H. Hosono, J. Am. Chem. Soc. **130**, 3296 (2008).
[2] Z. A. Ren, W. Lu, J. Yang, W. Yi, X. L. Shen, Z. C. Li, G. C. Che, X. L. Dong, L. L. Sun, F. Zhou, and Z. X. Zhao, Chin. Phys. Lett. **25**, 2215 (2008).
[3] T. Kroll, S. Bonhommeau, T. Kachel, H. A. Dürr, J. Werner, G. Behr, A. Koitzsch, R. Hübel, S. Leger, R. Schönfelder, A. K. Ariffin, R. Manzke, F. M. F. de Groot, J. Fink, H. Eschrig, B. Büchner, and M. Knupfer, Phys. Rev. B **78**, 220502(R) (2008).
[4] W. L. Yang, A. P. Sorini, C.-C. Chen, B. Moritz, W.-S. Lee, F. Vernay, P. Olalde-Velasco, J. D. Denlinger, B. Delley, J.-H. Chu, J. G. Analytis, I. R. Fisher, Z. A. Ren, J. Yang, W. Lu, Z. X. Zhao, J. van den Brink, Z. Hussain, Z.-X. Shen, and T. P. Devereaux, Phys. Rev. B **80**, 014508 (2009).
[5] V. I. Anisimov, E. Z. Kurmaev, A. Moewes, and I. A. Izyumov, Physica C **469**, 442 (2009).
[6] K. Haule, J. H. Shim, and G. Kotliar, Phys. Rev. Lett. **100**, 226402 (2008).
[7] L. Hozoi and P. Fulde, Phys. Rev. Lett. **102**, 136405 (2009).
[8] E. Z. Kurmaev, R. G. Wilks, A. Moewes, N. A. Skorikov, Yu. A. Izyumov, L. D. Finkelstein, R. H. Li, and X. H. Chen, Phys. Rev. B **78**, 220503(R) (2008).
[9] W. Malaeb, T. Yoshida, T. Kataoka, A. Fujimori, M. Kubota, K. Ono, H. Usu, K. Kuroki, R. Arita, H. Aoki, Y. Kamihara, M. Hirano, and H. Hosono, J. Phys. Soc. Jpn. **77**, 093714 (2008).
[10] F. Bondino, E. Magnano, M. Malvestuto, F. Parmigiani, M. A. McGuire, A. S. Sefat, B. C. Sales, R. Jin, D. Mandrus, E. W. Plummer, D. J. Singh, and N. Mannella, Phys. Rev. Lett. **101**, 267001 (2008).
[11] A. Koitzsch, D. Inosov, J. Fink, M. Knupfer, H. Eschrig, S. V. Borisenko, G. Behr, A. Köhler, J. Werner, B. Büchner, R. Follath, and H. A. Dürr, Phys. Rev. B **78**, 180506(R) (2008).

[12] L. H. Tjeng, C. T. Chen, J. Ghijsen, P. Rudolf, and F. Sette, Phys. Rev. Lett. **67**, 501 (1991).
[13] S. Hüfner, Adv. Phys. **43**, 183 (1994).
[14] A. Fujimori, M. Saeki, N. Kimizuka, M. Taniguchi, and S. Suga, Phys. Rev. B **34**, 7318 (1986).
[15] A. Fujimori, N. Kimizuka, M. Taniguchi, and S. Suga, Phys. Rev. B **36**, 6691 (1987).
[16] C. Guillot, Y. Ballu, J. Paigné, J. Lecante, K. P. Jain, P. Thiry, R. Pinchaux, Y. Pétroff, and L. M. Falicov, Phys. Rev. Lett. **39**, 1632 (1977).
[17] M. Weinelt, A. Nilsson, M. Magnuson, T. Wiell, N. Wassdahl, O. Karis, A. Föhlisch, N. Mårtensson, J. Stöhr, and M. Samant, Phys. Rev. Lett. **78**, 967 (1997).
[18] S. Hüfner, S.-H. Yang, B. S. Mun, C. S. Fadley, J. Schäfer, E. Rotenberg, and S. D. Kevan, Phys. Rev. B **61**, 12582 (2000).
[19] A. Föhlisch, O. Karis, M. Weinelt, J. Hasselström, A. Nilsson, and N. Mårtensson, Phys. Rev. Lett. **88**, 027601 (2002).
[20] G. L. Sun, D. L. Sun, M. Konuma, P. Popovich, A. Boris, J. B. Peng, K.-Y. Choi, P. Lemmens, and C. T. Lin, arXiv:0901.2728 (unpublished).
[21] H. Eschrig and K. Koepernik, Phys. Rev. B **80**, 104503 (2009).
[22] J. J. Yeh and I. Lindau, At. Data Nucl. Data Tables **32**, 1 (1985).
[23] M. Rotter, M. Tegel, D. Johrendt, I. Schellenberg, W. Hermes, and R. Pöttgen, Phys. Rev. B **78**, 020503(R) (2008).
[24] S. Hüfner, *Photoelectron Spectroscopy* (Springer, New York, 1996).
[25] G. B. Armen and H. Wang, Phys. Rev. A **51**, 1241 (1995).
[26] G. van der Laan, C. Westra, C. Haas, and G. A. Sawatzky, Phys. Rev. B **23**, 4369 (1981).
[27] T. Kroll, F. Roth, A. Koitzsch, R. Kraus, D. R. Batchelor, J. Werner, G. Behr, B. Buechner, and M. Knupfer, New J. Phys. **11**, 025019 (2009).
[28] $\Delta=0$ refers to the center of gravity of the d^6 and d^7L multiplets. $\Delta=1.25$ eV (as used in Ref. 3) refers to the lowest energy levels of the d^6 and d^7L multiplets.
[29] S. de Jong, Y. Huang, R. Huisman, F. Massee, S. Thirupathaiah, M. Gorgoi, F. Schaefers, R. Follath, J. B. Goedkoop, and M. S. Golden, Phys. Rev. B **79**, 115125 (2009).
[30] S. Doniach and M. Sunjic, J. Phys. C **3**, 285 (1970).
[31] J. A. Leiro and M. H. Heinonen, Phys. Rev. B **59**, 3265 (1999).
[32] F. M. F. de Groot, Coord. Chem. Rev. **249**, 31 (2005).